Materials Transactions, Vol. 49, No. 8 (2008) pp. 1900 to 1904
©2008 The Japan Institute of Metals
EXPRESS REGULAR ARTICLE

Optimization of Zr-Doped ZnO Thin Films Prepared by Sol-Gel Method

Chien-Yie Tsay* and Kai-Shiung Fan

Department of Materials Science and Engineering, Feng Chia University, Taichung, Taiwan 40724, R.O. China

Semiconductor thin films of Zr-doped ZnO, with Zr concentrations varying from 0 to 5 at%, have been prepared using a sol-gel method. Crystallinity, microstructure, and optical properties affected by Zr concentration were investigated. In this study, Zr-doped ZnO thin films were deposited onto alkali-free glass substrates by spin-coating. The as-deposited films were preheated at 300°C and then annealed at 500°C in air. The experimental results showed that doping ZnO thin films with Zr not only refined the grain size but also increased transmittance and resistivity. Among all the thin films investigated in the present study, the 3 at% Zr-doped ZnO thin film exhibited the best properties with a transmittance of 86.3% and a RMS roughness value of 5.86 nm. In addition, thin-film transistors were fabricated by spin-coating a 3 at% Zr-doped ZnO active channel layer onto a transistor subassembly. These transistors exhibited n-type depletion mode in which threshold voltage and drain current on-to-off ratio were −18.0 V and 9.6×10^5, respectively. [doi:10.2320/matertrans.MER2008111]

(Received April 4, 2008; Accepted May 28, 2008; Published July 9, 2008)

Keywords: *oxide semiconductors, zinc oxide, thin films, zirconium doping, sol-gel method*

1. Introduction

Polycrystalline oxide semiconductors have attracted considerable interest for photovoltaic devices and optical-electrical devices. Among these materials, zinc oxide (ZnO) is a promising candidate for transparent thin film transistors (TTFTs) in active matrix liquid crystal displays (AMLCDs)[1] and flexible displays.[2] ZnO exhibits non-toxicity, high transparency and a wide range of conductivity levels from metallic to insulating. Its unique electrical and optical properties have made it popular in piezoelectric transducers, surface acoustic wave (SAW) devices, laser diodes, photoconductive UV detectors, gas sensors, etc. Several reports[3–5] have indicated that ZnO TFTs exhibited a high off-current (I_{off}) and a low on-to-off current ratio because a transistor with an active channel layer made from undoped ZnO film has a high carrier density that causes the channel to conduct when an applied gate voltage is absent. It has been demonstrated that the electrical characteristics of ZnO films can be controlled by doping with ternary elements[6,7] or by heat treatment processes.[8,9]

ZnO-based thin films have been prepared by various thin film deposition techniques, such as RF/DC magnetic sputtering deposition, pulsed laser deposition, chemical vapor deposition, chemical bath deposition, spray pyrolysis, sol-gel methods, etc. Use of solution-based processes to form oxide semiconductors may improve the manufacturing throughput of microelectrical devices by enabling maskless processes, including inkjet printing,[10] selective electroless plating,[11] etc. Solution-based processes such as sol-gel spin coating[8,12,13] have attracted investigation for use in transparent electronic devices.[14,15] Spin coating is a simple, low cost and large area thin-film coating method that is simpler than vacuum deposition techniques (PVD or CVD).

In a previous study it was demonstrated that Mg incorporated within ZnO films can serve as the active channel layer for TFTs and the on/off current ratios of pure ZnO and $Zn_{0.8}Mg_{0.2}O$ TFTs are 10 and 10^6, respectively.[16] A ZnO channel layer that incorporates 20 at% Mg can improve on/off current ratio by five orders of magnitude. However, for films that incorporate 20 at% Mg, the off-current increases as applied gate voltage (V_G) goes from −50 to −80 V. The ionic radius of Zr^{+4} (0.8 Å) is larger than Zn^{+2} (0.74 Å). Doping ZnO films with Zr decreases carrier concentration[5] and improves transparency in the visible range.[17] In the present study, polycrystalline semiconductor thin films of Zr-doped ZnO were prepared by a sol-gel method and the effects of Zr concentration on crystallinity, microstructure, surface roughness, and transparency were studied. Moreover, TFTs with a 3 at% Zr-doped ZnO ($Zn_{0.97}Zr_{0.03}O$) active channel layer were fabricated and their electrical characteristics were evaluated.

2. Experimental

Four batches of Zr-doping ZnO sols were prepared with concentrations of Zr dopant of 0, 1, 3 and 5 at%. Zinc acetate dehydrate and zirconium acetate hydrate were dissolved in 2-methoxyethanol, and then monoethanolamine (MEA) was added to the solution as a stabilizer. The molar ratio of MEA to metal ions in the as-prepared sols was maintained at 1.0 and the concentration of metal ions was controlled at 0.75 mole/L. Each complex solution was stirred for 2 h at 60°C to yield a transparent and homogenous sol. All Zr-doped ZnO (ZZO) films were coated onto alkali-free glass (Corning 1737, $5 \times 5\,cm^2$) using spin coating at a speed of 2500 rpm for 20 seconds. The as-coated films were preheated at 300°C for 10 minutes to evaporate the solvent and to burn out organic composites. After the coating procedure had been repeated three times, the films were annealed in a tube furnace at 500°C for 1 h.

After the ZZO films had been annealed, their crystallinity was determined by X-ray diffractometry (XRD, MAC Science MAXP3, Japan). Surface morphology and a cross-sectional view of each ZZO film were observed using field-emission scanning electron microscopy (FE-SEM, HITACHI S-4800, Japan). Surface roughness was measured using scanning probe microscopy (SPM, Digital Instrument NS4/D3100CL, Germany). The resistivity and optical transmittance of each film were measured by a high resistivity

*Corresponding author, E-mail: cytsay@fcu.edu.tw

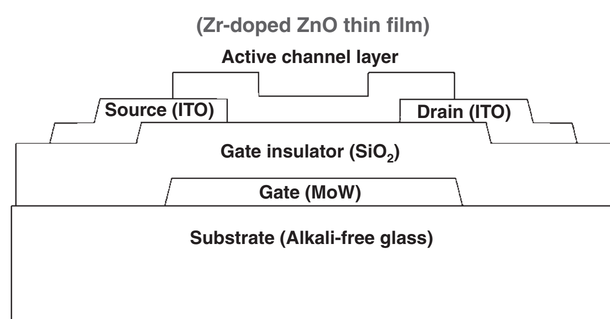

Fig. 1 Schematic cross-sectional structure of TFT with Zr-doped ZO active channel layer.

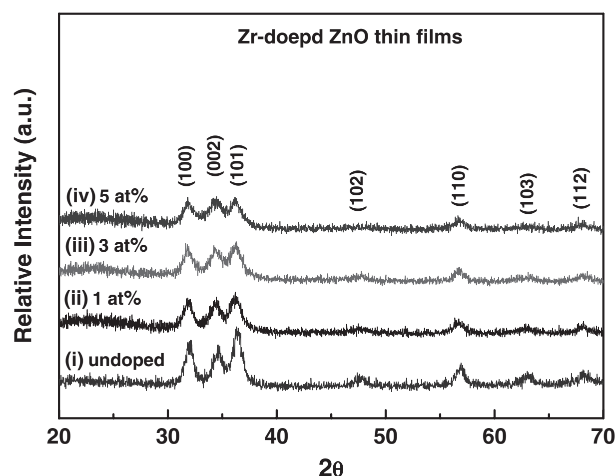

Fig. 2 X-ray diffraction patterns of Zr-doped ZnO thin films annealed in air at 500°C for 1 h.

Table 1 Microstructure, optical properties and resistivity of Zr-doped ZnO thin films.

Zr concentration (at%)	Average crystallite size (nm)	Lattice parameters (Å) *a*-axis	Lattice parameters (Å) *c*-axis	RMS roughness (nm)	Transmittance* (%)	Bandgap (eV)	Resistivity (Ω-cm)
0	9.2	3.227	5.189	16.66	81.9	3.22	2.6×10^3
1	8.4	3.235	5.200	15.03	84.9	3.23	4.3×10^3
3	8.2	3.245	5.215	5.86	86.3	3.24	3.6×10^4
5	7.1	3.247	5.218	6.15	86.0	3.23	6.6×10^4

*This table only gives transmittances for a wavelength of 550 nm.

meter (MCP-HT450, DIA INSTRUMENTS CO., LTD, Japan) and a spectrophotometer (Mini-D2T, Ocean Optics Inc., USA), respectively.

Film thickness uniformity, surface roughness, resistivity and other characteristics were evaluated to choose an optimum ZZO film, which was appraised for use as the active channel layer of a TFT. A simple bottom-gate TFT was fabricated by a hybrid method that combined the standard micro-electrical fabrication process and the sol-gel spin coating method. Figure 1 shows a schematic of the TFT with a ZZO active layer. A molybdenum tungsten alloy (MoW) thin film with a thickness of 100 nm was deposited and patterned onto an alkali-free glass substrate; it served as the bottom gate electrode. Silicon dioxide (SiO_2) film, with a thickness of 300 nm, was prepared by plasma enhanced chemical vapor deposition (PECVD), and served as the gate insulator. The source and drain electrodes were indium tin oxide (ITO) thin film with a thicknesses of 100 nm that was deposited by sputtering, and then patterned by a conventional photolithography process. The channel length and width of the TFT device were offset by 500 and 10 μm, respectively. Finally, the ZZO semiconductor thin film was deposited onto the multilayer structure by spin coating. The resulting ZZO TFT was evaluated for current-voltage (*I*-*V*) characteristics in a darkroom using a semiconductor parameter analyzer (HP 4155B, USA).

3. Results and Discussion

Our previous study has demonstrated that Mg incorporated within a ZnO film can serve as the active channel layer for a TFT and that the $Zn_{0.8}Mg_{0.2}O$ TFTs exhibited the best electrical characteristics among the Mg incorporated ZnO films.[18] However, the off current increased from 10^{-12} to 10^{-9} A when the gate voltage went from -50 to -100 V. This electrical characteristic may not be acceptable for commercial applications. In the present study, Zr-doped ZnO thin films were prepared and examined for use in TFTs.

The crystal structure of these ZZO thin films was identified by X-ray diffraction. Figure 2 shows the XRD patterns of undoped and Zr-doped ZnO thin films. Crystallized ZnO exhibits a hexagonal wurzite structure which is confirmed by three main diffraction peaks for the (100), (002) and (101) planes (Zincite, JCPDS 36-1451). It can be noted that, from the XRD patterns, the intensities of diffraction peaks decrease with increasing Zr concentration (curves (ii)–(iv) in Fig. 2). The average crystallite size (d) of each of the ZZO films was estimated using Scherrer's formula:[19]

$$d = \frac{0.9\lambda}{B\cos\theta_B}, \tag{1}$$

where λ is the X-ray wavelength of 1.54 Å, θ_B is the Bragg diffraction angle and B is the FWHM (full width at half maximum) of θ_B. The calculated average crystallite sizes of these ZZO films, summarized in Table 1, were 9.2, 8.4, 8.2 and 7.1 nm for undoped, 1, 3 and 5 at% Zr doping, respectively. It can be noted that Zr-doped ZnO thin films have reduced average crystallite sized. It was observed that the (001) and (002) peaks slightly shifted towards the lower diffraction angle after Zr doping. The *a*- and *c*-lattice parameters calculated from these peaks are presented in Table 1. It has been found that Zr doping can increase the *a*-

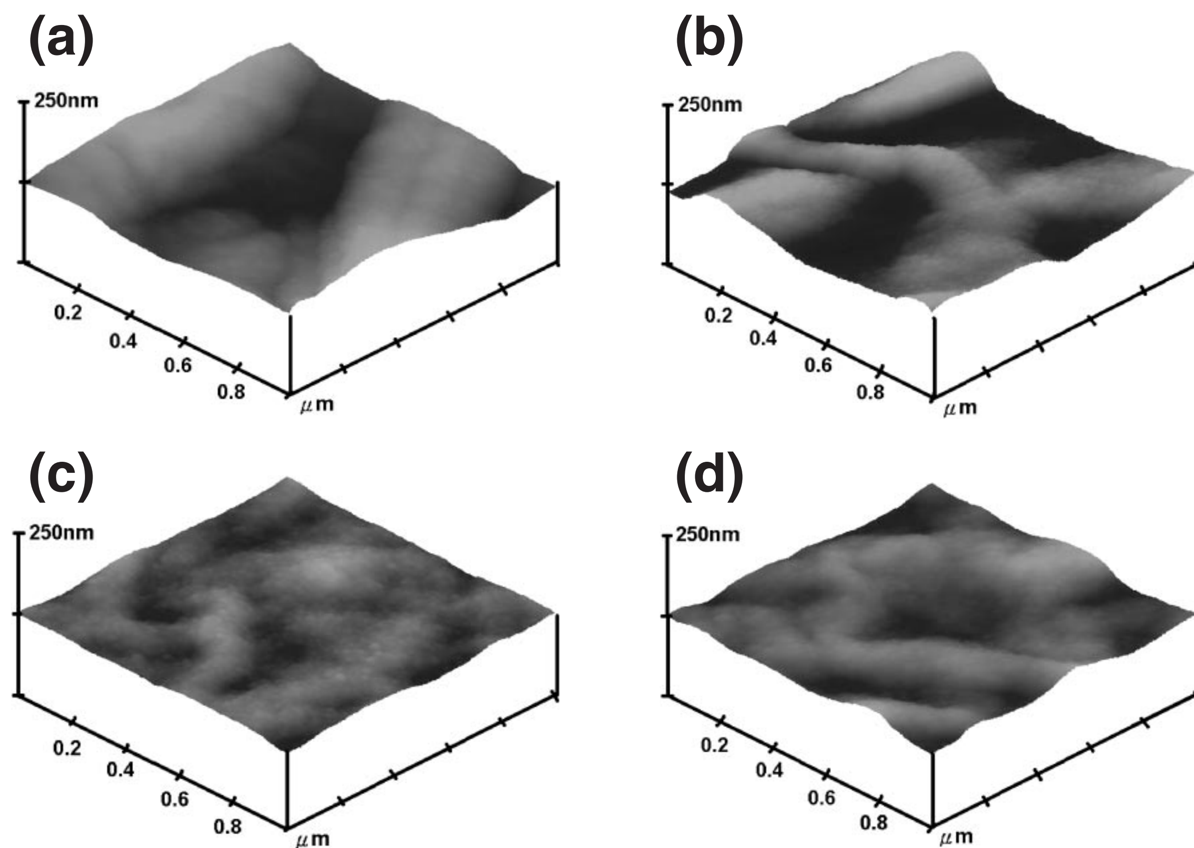

Fig. 3 SPM images of Zr-doped ZnO thin films: (a) undoped, (b) 1 at%, (c) 3 at%, and (d) 5 at% Zr-doped samples.

and *c*-lattice parameters of ZnO films. The *a*- and *c*-lattice parameters are 3.227 Å and 5.189 Å for pure ZnO films, and increase gradually to maxima of 3.247 Å and 5.218 Å for 5 at% ZZO films. The ionic radius of Zr^{4+} (0.8 Å) is larger than that Zn (0.74 Å). For this reason, Zr doping can increase the lattice parameters of unit cells. This study shows a similar trend to that reported in the literature.[17)]

The four surface morphologies in Fig. 3 show the influence of the Zr doping in these ZnO thin films. As shown in Fig. 3(a), the undoped ZnO film can have fiber-like structures. Figures 3(b) to 3(d) show an improvement in surface flatness with Zr doping. It is suggested that Zr doping decreases average crystallite size in ZnO films, resulting in improved surface flatness. The values of RMS roughness of the ZZO films, given in Table 1, show that RMS roughness decreased with doping concentrations up to 3 at% Zr and increased at 5 at%. That is, the 3 at% Zr-doped ZnO thin film exhibited the smallest RMS value (5.86) among all of the annealed ZZO thin films investigated in this study. Cross-sectional views of the undoped ZnO and 3 at% Zr-doped ZnO films are shown in Figs. 4(a) and 4(b), respectively, to illustrate the differences in microstructure and film thickness. The thicknesses of both undoped ZnO and 3 at% ZZO films are ~170 nm. The pictures also reveal that Zr doping in ZnO films can markedly reduce the average grain size; this finding agrees with XRD measurements.

The optical transmittance spectra of the ZZO films, with wavelengths from 200 to 800 nm, are shown in Fig. 5. All ZZO samples were found to exhibit sharp absorption edges in the UV region. This absorption edge slightly shifted to the

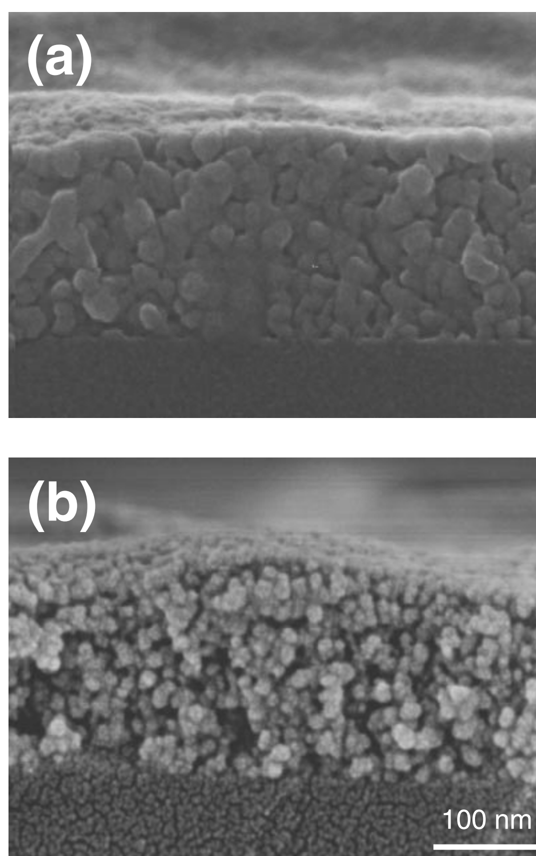

Fig. 4 SEM micrographs of cross-section of Zr-doped ZnO thin films: (a) undoped and (b) 3 at% Zr-doped samples.

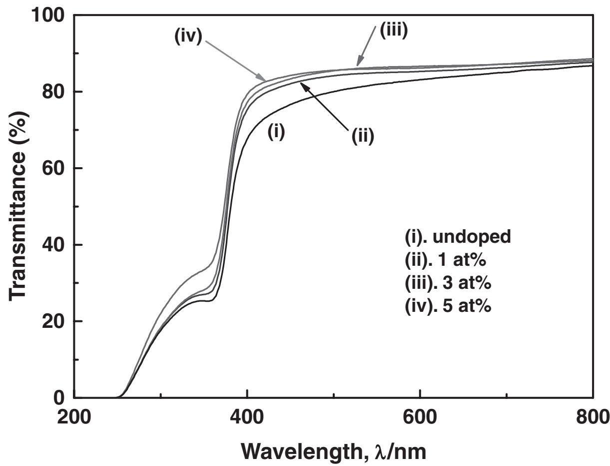

Fig. 5 Optical transmittance spectra of undoped and Zr-doped ZnO thin films.

left (i.e., shorter wavelengths) when Zr was doped into the ZnO film. Tan *et al.* proposed that the absorption edge blueshift was due to the poor crystallinity of ZnO thin films.[20] The transmittances for a wavelength of 550 nm, listed in Table 1, reveal that Zr-doped films exhibited better transparency (from 84.9–86.3%) than that of the pure ZnO film (81.9%). Among the films investigated in the present study, the $Zn_{0.97}Zr_{0.03}O$ film exhibited the best transparency, namely 86.3%. According to Lee *et al.*, surface morphology has a strong influence on the transparency properties of ZnO films.[21] The result of the present study is in good agreement with the way in which the values of surface roughness vary with Zr doping concentration.

The Tauc model can obtain the optical bandgaps of ZZO thin films from their absorption edges:[22]

$$\alpha(h\nu) = A(h\nu - E_g)^n, \qquad (2)$$

where α is the absorption coefficient, $h\nu$ is the photon energy, A is a constant and E_g is the optical bandgap. For a direct bandgap material, such as a ZnO-based thin film, $n = 1/2$ is the most suitable value. The absorption coefficient (α) in the UV region of these Zr-doped ZO thin films can be calculated from $I = I_o e^{-\alpha t}$,[23] where I is intensity of the transmitted light, I_o is the intensity of incident light and t is the thickness of the ZZO films. The bandgap values were extrapolated from the straight sections of the plot of $(\alpha h\nu)^2$ versus photo energy ($h\nu$). Table 1 lists the bandgap (E_g) values of ZZO films; it shows that bandgaps increase slightly for ZnO films doped with Zr. The bandgaps of Zr-doped ZnO thin films are larger than those of undoped thin films; the effect of average crystallite sizes may explain this.[20]

Previous discussions have mentioned that ZnO exhibits wide-range conductivity and that its electrical characteristics can be controlled by doping ternary elements. Table 1 shows the resistivity values of ZZO films with various Zr concentrations. It can be noted that the resistivities of ZZO films increased by one order of magnitude when the amount of dopant was greater than 3 at%. Paul *et al.*[24] have indicated that increased dopant atoms form neutral defects which do not contribute free electrons and which result in a decrease in carrier concentration.

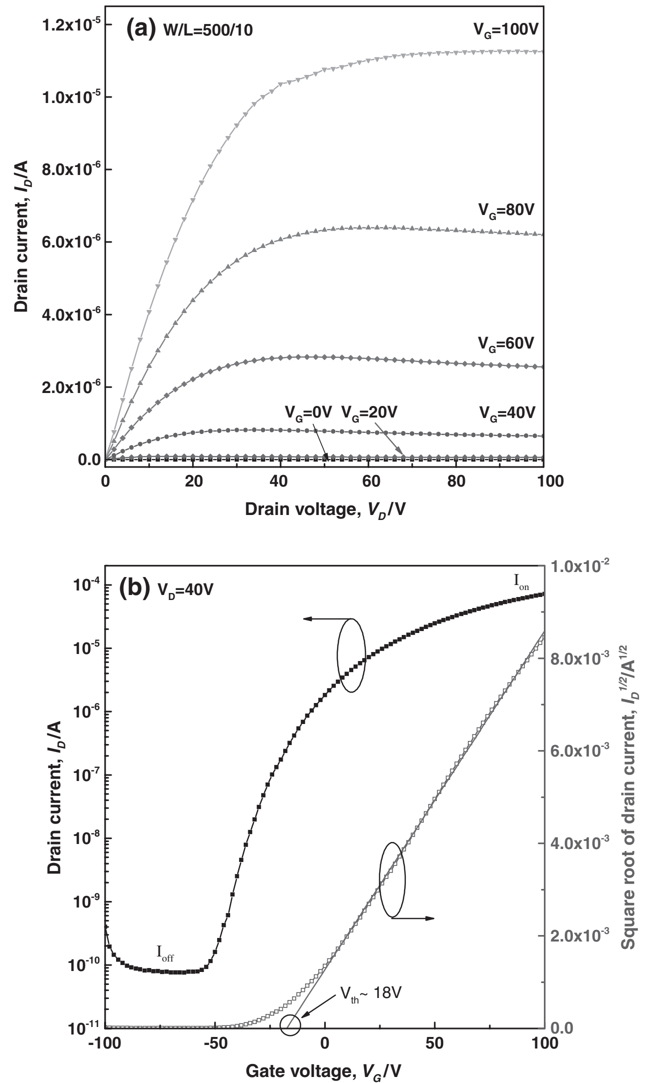

Fig. 6 (a) I_D-V_D curves and (b) I_D-V_G curves of TFT using the 3 at% Zr-doepd ZnO thin film as the active channel layer.

According to the above characterizations, the 3 at% Zr-doped ZnO thin film exhibited good performance. Moreover, a previous report found that the mobility of 3 at% ZZO film was two times higher than that pure ZnO film.[24] Therefore, TFTs with a 3 at% ZZO active channel layer were fabricated and their current-voltage (*I-V*) characteristics were evaluated. Figure 6(a) shows the drain current-drain voltage (I_D-V_D) curves for a $Zn_{0.97}Zr_{0.03}O$ TFT. It shows that the TFT operates as an n-channel device and that the drain current increases with positive gate bias. Furthermore, each I_D curve has a flat slope and exhibits current saturation for a large V_D region. The oxide semiconductor films fabricated by solution-based processes have inferior quality compared to films deposited by vacuum deposition techniques. For this reason, sol-gel derived ZZO channel layer located on a transferring path of a carrier would cause this TFT to exhibit larger gate bias than would be caused by the active channel of a ZnO-based TFT deposited by sputtering or pulsed laser deposition.[25,26] Figure 6(b) shows the I_D-V_G curves of the same device, which was measured at a fixed drain voltage (V_D) of 40 V. This I_D-V_G curve reveals that the off-current was about 10^{-10} A with V_D between -50 to -80 V and a 9.6×10^5 on-

to-off current ratio. The threshold voltage (V_{th}) was derived from the $(I_D)^{1/2}$-V_G plot. By fitting a straight line and then intercepting the *x*-axis, a V_{th} of -18 V can be obtained; this indicates that the 3 at% ZZO TFT operates in depletion mode.

4. Conclusions

Polycrystalline semiconductor thin-films of ZnO doped with Zr were prepared on glass substrates by a sol-gel spin coating process. The as-deposited films were annealed in air at 500°C for 1 h. ZnO thin films doped with Zr had obviously improved transparency in the visible range, decreased surface roughness, and degenerated crystallization. Among the ZZO films investigated in this study, the $Zn_{0.97}Zr_{0.03}O$ films exhibited the best optical transmittance, 86.3%, the minimum RMS roughness, 5.86 nm and a resistivity of 3.6×10^4 Ω-cm. Moreover, the results demonstrated that semiconducting $Zn_{0.97}Zr_{0.03}O$ film can serve as the active channel layer of a TFT. In n-channel depletion mode, the $Zn_{0.97}Zr_{0.03}O$ TFT exhibited a threshold voltage of -18.0 V and an on/off current ratio of 9.4×10^5.

Acknowledgments

This work was supported by the National Science Council of Republic of China under Contract No. NSC 95-2221-E-035-006 and the Taiwan TFT-LCD Association (TTLA) under Contract No. A643TT1000-S21. The authors also acknowledge Mr. S. H Chiang and Mr. C. C. Yu (R. D. engineering of TTLA) for the experiments assistance.

REFERENCES

1) T. Hirao, M. Furuta, H. Furuta, T. Matsuda, T. Hiramatsu, H. Hokari, M. Yoshida, H. Ishii and M. Kakegawa: J. SID. **15** (2007) 17–22.
2) A. N. Banerjee, C. K. Ghosh, K. K. Chattopadhyay, H. Minoura, A. K. Sarkar, A. Akiba, A. Kamiya and T. Endo: Thin Solid Films. **496** (2006) 112–116.
3) S. K. Park, C. S. Hwang, H. Y. Jeong, H. Y. Chu and K. I. Cho: Electrochem. Solid-State Lett. **11** (2008) H10–H14.
4) K. Remashan, D. K. Hwang, S. D. Park, J. W. Bas, G. Y. Yeom, S. J. Park and J. H. Jang: Electrochem. Solid-State Lett. **11** (2008) H55–H59.
5) J. H. Lee, P. Lin, J. C. Ho and C. C. Lee: Electrochem. Solid-State Lett. **9** (2006) G117–G120.
6) S. M. Lukas and M. D. Judith: Materials Today **10** (2007) 40–48.
7) D. Karmakar, I. Dasgupta, G. P. Das and Y. Kawazoe: Mater. Trans. **48** (2007) 2119–2122.
8) B. J. Norris, J. Anderson, J. F. Wager and D. A. Keszler: J. Phys. D: Appl. Phys. **36** (2003) L105–L107.
9) M. Wang, J. Wang, W. Chen, Y. Cui and L. Wang: Mater. Chem. Phys. **97** (2006) 219–225.
10) D. H. Lee, Y. J. Chang, W. Stickle and C. H. Chang: Electrochem. Solid-State Lett. **10** (2007) K51–H54.
11) C. Y. Tsay, C. K. Lin, H. M. Lin, S. C. Chang and B. C. Chung: Mater. Sci. Foru. **561–565** (2007) 1165–1168.
12) Y. J. Chang, D. H. Lee, G. S. Herman and C. H. Chang: Electrochem. Solid-State Lett. **10** (2007) H135–H138.
13) B. S. Ong, C. Li, Y. Li, Y. Wu and R. Loutfy: J. Am. Chem. Soc. **129** (2007) 2750–2751.
14) J. F. Wager: Science **300** (2003) 1245–1246.
15) E. Fortunato, P. Barquinha, A. Pimentel, A. Goncalves, A. Marques, L. Pereira and R. Martins: Thin Solid Films **487** (2005) 205–211.
16) J. H. Lee, P. Lin, C. C. Lee, J. C. Ho and Y. W. Wang: Jpn. J. Appl. Phys. **44** (2005) 4784–4789.
17) S. B. Qadri, H. Kim, J. S. Horwitz and D. B. Chrisey: J. Appl. Phys. **88** (2000) 6564–6566.
18) C. Y. Tsay, M. C. Wang and S. C. Chiang: Mater. Trans. **49** (2008) 1186–1191.
19) B. D. Cullity and S. R. Stock: *Elements of X-ray Diffraction*, (Prentice-Hall, Inc, New Jersey, 2001) pp. 388.
20) S. T. Tan, B. J. Chen, X. W. Sun, W. J. Fan, H. S. Kwok, X. H. Zhang and S. J. Chua: J. Appl. Phys. **98** (2005) 013505.
21) J. H. Lee and B. O. Park: Thin Solid Films **426** (2003) 94–99.
22) J. Tauc, R. Grigorovici and A. Vancu: Phys. Stat. Sol. **15** (1966) 627–637.
23) R. D. Tarey and T. A. Raju: Thin Solid Films **128** (1985) 181–189.
24) G. K. Paul, S. Bandyopadhyay, S. K. Sen and S. Sen: Mater. Chem. Phys. **79** (2003) 71–75.
25) H. H. Hsieh and C. C. Wu: Appl. Phys. Lett. **89** (2006) 041109.
26) P. K. Shin and Y. Aya, T. Ikegami and K. Ebihara: Thin Solid Films **516** (2008) 3767–3771.